Non-Gaussian and Cooperative Dynamics of Entanglement Strands in Polymer Melts

Margarita Kruteva*[1], Michaela Zamponi[2], Ingo Hoffmann[3], Jürgen Allgaier[1], Michael Monkenbusch[1], Dieter Richter[1]

[1] Forschungszentrum Jülich GmbH, Jülich Centre for Neutron Science (JCNS-1: Neutron Scattering and Biological Matter), 52425 Jülich, Germany

[2] Forschungszentrum Jülich GmbH, Jülich Centre for Neutron Science at MLZ, Lichtenbergstraße 1, 85748 Garching, Germany

[3] Institut Laue-Langevin (ILL), B.P. 156, F-38042 Grenoble Cedex 9, France

For Table of Contents Only

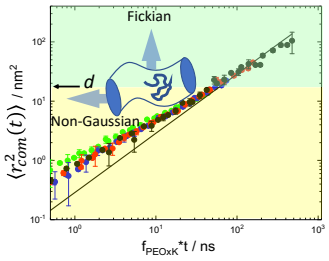

Abstract

We present a study on tracer diffusion of short poly(ethylene oxide) (PEO) tracers in a strongly entangled PEO melt. We find that within the entanglement volume, the dynamics of the entanglement strands is significantly Non-Gaussian. Following theoretical predictions of Guenza (M. Guenza, *Phys. Rev. E*, **89** (5) 052603 (2014)) we quantify the Non-Gaussian correction $\alpha_2(t)$ in terms of a logarithmic Gaussian function with a maximum at a time in the order of the Rouse times of the different tracers and a width that is independent of the tracer's length. The strength of the Non-Gaussian correction is found to be equal for all tracers providing another proof that the tracers mirror the host dynamics, which needs to be

* Corresponding author. E-mail: m.kruteva@fz-juelich.de

independent of the tracer length. As for polyethylene (M. Zamponi *et al.*, *Phys. Rev. Lett.* , **126** (18), 187801 (2021)), independent of their molecular weight, the tracer's center-of-mass mean square displacements are sub-diffusive at short times until they have reached the size of the reptation tube d; then, a crossover to Fickian diffusion takes place indicating cooperative chain motion within the entanglement volume d^3. Thus, the host dynamics within the tube is not only cooperative but also significantly Non-Gaussian.

Introduction

The research on Non-Gaussian (NG) dynamics in polymer melts has been largely focused on the decaging of polymer segments near the glass transition, where the deviations from a Gaussian displacement distribution was quantified in terms of the NG Parameter $\alpha_2(t)$[1]

$$\alpha_2(t) = \frac{3\langle[r_i(t)-r_i(0)]^4\rangle}{5\langle[r_i(t)-r_i(0)]^2\rangle^2} - 1 \qquad (1)$$

$r_i(t)$ denotes the position of segment "i" at time t. For Gaussian distributed displacements $\alpha_2(t) = 0$. The decaging process relates to the α-relaxation and exhibits a maximum near τ_α. Both extensive simulations [2–6] and experimental studies combined with simulations [7,8] were reported. The characteristic time τ_{α_2} for $\alpha_2(t)$ was found to relate non-linearly to τ_α: $\tau_{\alpha_2} \sim \tau_\alpha^{\cong 0.7}$ [9–11].

On the chain level, assuming monomer motion unperturbed by its neighbors, the dynamics of non-entangled shorter chains is commonly described by the Rouse model, where segmental friction and entropic forces drive the dynamics [12]. By molecular dynamics simulations in combination with neutron spin echo (NSE) observations on unentangled chains shortcomings of the Rouse model were related to intermolecular interactions [13]. From simulations Smith *et al.* [14] found that the monomer displacements are not distributed in a Gaussian fashion leading to a positive $\alpha_2(t)$. According to Smith's work and a significant amount of other simulation studies the NG behavior is accompanied by sub-diffusion of the non or very weakly entangled chains. In these short chain melts the cross over from sub-diffusivity to Fickian diffusion occurs

at about the Rouse time of the respective melt [14–21]. Based on NSE-experiments also Zamponi *et al.* [13] reported such behavior and could quantitatively describe these results in terms of generalized Langevin approach proposed by Guenza [22–26].

Equ. 2 describes the dynamic structure factor as a function of segment displacement $\langle r^2(t)\rangle$ including the NGP $\alpha_2(t)$. As is evident, a positive $\alpha_2(t)$ restricts the decay of $S(Q,t)$ relative to that of Gaussian distributed segment displacements at the same mean squared displacement (MSD).

$$S(Q,t) = exp\left\{-Q^2\frac{\langle r^2(t)\rangle}{6} + Q^4\alpha_2(t)\frac{\langle r^2(t)\rangle^2}{72}\right\} \quad (2)$$

For such chains Pan and Sun [4] have studied NG behavior by MD-simulations on coarse grained melts including chain stiffness effects. The evaluated $\alpha_2(t)$ display two maxima, a stronger one around the monomer decaging process and a second one in the Rouse like sub-diffusive regime that increases in strength with increasing chain stiffness. Hints for such weak Non-Gaussianities in the Rouse regime were already reported by M. Aichele *et al.* [9] who found some remaining Non-Gaussianity at the long time flank of $\alpha_2(t)$.

So far, these investigations into NG dynamics addressed non or weakly entangled polymer melts. Recently, based on simulations, Guenza investigated the NG behavior of entangled linear polymer melts [27]. For polyethylene (PE) she derived a function $\alpha_2(t)$ with the following features: (i) The dynamics is NG up to about the terminal times τ_R or τ_d for Rouse chains or entangled melts respectively; (ii) At a time that is smaller but proportional to the terminal time ($t \lesssim \tau_R$) $\alpha_2(t)$ exhibits a maximum; (iii) Its magnitude on the scale of the monomer depends on the chain length N as $\sqrt{N}$; (iv) Finally, the characteristic length scale of the dynamic heterogeneities is in the order of R_g, the size of the molecule.

Very recently, in order to sense the host dynamics on the level of the tube diameter d [28], we studied the dynamics of strongly entangled PE melts using a series of short non- or weakly entangled tracer PE-molecules. The chain motion was found to be caged within the entanglement volume d^3 rather than exhibiting unrestricted Rouse like chain relaxation as commonly supposed [12]. Also, compared to the Rouse prediction the amplitudes of the tracer's internal motion appeared to be significantly reduced. The origin of this behavior was related to the cooperativity of the tracer and host chains due to important interchain couplings. We note that the cooperativity of the tracer and long chain motion was observed to be restricted to the entanglement volume, beyond which the tracers performed Fickian diffusion.

In this work we present a study of poly(ethylene oxide) (PEO) tracer dynamics in strongly entangled PEO hosts. We address two aspects: 1. the transition of the diffusion from sublinear to Fickian at a MSD related to the tube diameter and 2. the Non-Gaussianity of the tracer Rouse dynamics. The modification of the Rouse dynamics is needed to consolidate the observed dynamic scattering with the model description of the tracer scattering function. In particular this is visible for the longer tracers. Motivated by the results of Guenza [27] in this paper we used her Ansatz for Non-Gaussianity for the tracer dynamics, which has a realistic physical background. We show that within the entanglement volume as in PE the melt dynamics is cooperative and in addition NG causing the apparent mode suppression. Thus, following Guenza cooperativity and Non-Gaussianity are the two sides of the same coin[27]. As tracers mirror the host dynamics, we demonstrate that cooperativity and Non-Gaussianity within the entanglement volume is not special to PE but appears to be a generic feature of strongly entangled polymer melts.

Theory

Non-Gaussian dynamics. The focus of this work is on the NG entanglement strand motion in strongly entangled polymer melts. Since short tracer chains move cooperatively with the host and mirror its dynamics (see Ref. [28] and PEO results presented later), here we use such tracers, in order to clarify the amount of Non-Gaussianity within the entanglement volume. Within this work we always deal with the chain dynamic structure factor, that is observed from labelled (hydrogenated) chains in a deuterated environment, and for simplicity name it "dynamic structure factor $S(Q,t)$". In $S(Q,t)$ the effect of NG displacement distributions in a first approximation shows up in the form of a NG correction as displayed in Equ. 2. While the interchain interaction and its consequences on the chain dynamics were treated theoretically by several authors, in particular by the Farago *et al.* [29], Guenza provided a treatable result for the dynamic structure factor of strongly entangled chains. Following her work, we describe the NG distribution of segmental motion in terms of $S(Q,t)$ as follows [27]:

$$S(Q,t) \cong \frac{1}{N} exp\left[-Q^2 \langle r_{com}^2(t)\rangle/6\right] \sum_{i,j}^{N} exp\left[-\left(\frac{Q^2}{6}\right) f(Q^2) \left\langle \left[r_i(t) - r_j(0)\right]^2 \right\rangle\right] \qquad (3)$$

with

$$f(Q^2) = 1 - Q^2 \alpha_2(t) \langle [r(t) - r(0)]^2 \rangle / 12 \qquad (4)$$

$\langle [r(t) - r(0)]^2 \rangle$ relates to the segment mean square displacement. For a Rouse chain we have [30]

$$\langle [r(t) - r(0)]^2 \rangle = \frac{1}{N} \frac{4N l_{seg}^2}{\pi^2} \sum_{m,p=1}^{N} \frac{1}{p^2} cos\left(\frac{p\pi m}{N}\right)^2 \left[1 - exp\left\{-2W\left(1 - cos\left(\frac{p\pi}{N}\right)\right) t\right\}\right] \qquad (5a)$$

$$\left\langle \left[r_i(t) - r_j(0)\right]^2 \right\rangle = 6D(t)t + |i-j|l_{seg}^2 +$$

$$+ \frac{4Nl_{seg}^2}{\pi^2} \sum_{p=1}^{N} \frac{1}{p^2} cos\left(\frac{p\pi j}{N}\right) cos\left(\frac{p\pi i}{N}\right) \left[1 - exp\left(\frac{tp^2}{\tau_R}\right)\right] \quad (5b)$$

where W is the Rouse rate and l_{seg} the segment length. We note that a proper theory would need to generalize the Rouse equations for interchain interactions involving *e.g.* a memory function formalism [31] . This, however, is well beyond this experimental work.

The center-of-mass mean squared displacement $\langle r_{com}^2(t)\rangle$ was taken as a sequence of two power laws $\langle [r_{com}^2(t) - r_{com}^2(0)]^2\rangle \sim t^\beta$ for $\langle r_{com}^2(t)\rangle \leq \langle r_{cross}^2\rangle$ and $\langle r_{com}^2(t)\rangle \sim t$ for larger MSD, where $\langle r_{cross}^2\rangle$ describes the cross over from sub-diffusivity to Fickian diffusion.

$$exp\left[-Q^2 \langle r_{com}^2(t)\rangle/6\right] = exp\left(-\frac{Q^2}{6} \left[\left\{ e^{-ln\left(1/6 \frac{\langle r_{cross}^2\rangle}{D_{tr}}\right)^\beta \langle r_{cross}^2\rangle t^\beta} \right\}^a + (6D_{tr}t)^a \right]^{1/a} \right) \quad (6)$$

with $a = 8$ controlling the sharpness of the transition from sublinear (exponent $\beta \simeq 0.7 \cdots 0.8$) to linear diffusion with constant D_{tr} at MSD $\langle r_{cross}^2\rangle$.

What remains is to find an expression for $\alpha_2(t)$. Following the results of Guenza we use a logarithmic Gaussian function

$$\alpha_2(t) = \alpha_0 exp\left[-\left\{\left(ln(t) - ln(t_{max})\right)^2 / 2\,\sigma^2\right\}\right] \quad (7)$$

at $t_{max}:\ \alpha_2(t_{max}) = \alpha_0;\ t_{max}$, thereby, is proportional to the Rouse times of the different tracers, respectively. In the scattering function a positive $\alpha_2(t)$ reduces the apparent Rouse mode contributions in $S(Q,t)$. Thus, NG dynamics might also be behind the weak Rouse

contribution to $S(Q,t)$ for the tracer dynamics in PE melts [28] and could offer an understanding, why such strongly reduced Rouse contributions to the tracer dynamic structure factors were found.

Non interacting dynamic multi-component RPA. In a blend of short and long chains the random phase approximation (RPA) corrections are not only necessary to describe the static structure factor, but even more important for modelling the dynamics of short chains in the presence of long chains. The dynamic structure factor of the short chains contains contributions from the slow long chain dynamics that needs to be corrected for. Akcasu and Tombakoglu derived expressions for the dynamic scattering function of a multicomponent $(n+1)$ polymer system in the framework of the RPA[32]. The result is given in form of Laplace transforms:

$$\boldsymbol{S}(Q,s) = [\mathbf{1}s + Q^2\boldsymbol{D}(Q,s)]^{-1}\boldsymbol{S}(Q) \tag{8}$$

where $\boldsymbol{S}(Q,s)$ is the Laplace transformed scattering function, $\mathbf{1}$ the unity matrix and $\boldsymbol{D}(Q,s)$ a generalized diffusion matrix. Applying the contrast vector to the 2-dimensional scattering function matrix yields the observable intensity. The technical difficulty to apply this in practical evaluation schemes is the realization of the required Laplace transformations of the undisturbed functions and the back transformation of the results, to the time domain. In Ref. [33] we elaborated a practical scheme to perform this task including a software implementation[33]. In that work we also undertook a successful quantitative test of the procedure. The evaluation and fits in the present work are based on this procedure. They were also used and illustrated in the previous work on PE [28]. Finally, we note that the application of RPA corrections is merely a technical means to correct the scattering function for admixtures of the long chain scattering signal to the observed $S(Q,t)$ in the present contrast. It is

unavoidable that with finite concentration of the labelled component also the non-labeled (matrix) chains gain some visibility. This effect is well known for the static RPA corrections and appears to be even more important for systems of components with strongly asymmetric dynamics. In the dynamic scattering function $S(Q,t)$ a prominent feature of this admixture is a residual slowly decaying leveling at large t, where the scattering function of the short tracers has largely decayed already. This can clearly be seen directly (see Figures 1a,b and Figure S1) in the NSE data.

Experiment

Synthesis. The low molecular weight hydrogenous samples with M_n values of 1.00, 2.11, 3.16, and 4.53 kg/mol were obtained from Sigma-Aldrich and used as received. The high molecular weight hydrogenous and deuterated PEO samples were synthesized as described in Ref. [34], except that for the hydrogenous polymer potassium metalated PEO2K and for the deuterated polymer potassium *tert*-butoxide were used as initiators [34]. The potassium metalated PEO2K was synthesized from PEO2K and 1.9-Eq. of potassium *tert*-butoxide in dry toluene at 60°C. After mixing the ingredients inside a glove box, the solvent and the *tert*-butanol formed were removed under high vacuum conditions. Deuterated ethylene oxide was obtained from Cambridge Isotope Laboratories (isotopic purity 98%) and purified as described in Ref. [34]. M_w and M_w distributions were measured by SEC/LS, except for the low molecular weight hydrogenous samples, where M_n values were determined by ^{1}H-NMR in deuterated pyridine (see Ref. [34]) and M_w/M_n values were measured by conventional SEC calibrated with PEO standards. The polydispersities are displayed in Table 1. The molecular weight of the long chain PEO matrix was 42.9 kg/mol with $M_w/M_n = 1.01$. Each sample contained 5%

hydrogenous tracer molecules in the deuterated PEO matrix. The sample characteristics are given in Table 1. Furthermore, hydrogenous long chains (42.8 kg/mol M_w/M_n=1.01) were synthesized.

Table 1: Molecular weight M_n; number of monomers N; polydispersity M_w/M_n,; the number of entanglement $Z = M_n/M_e$ with M_e=2.1 kg/mol the entanglement molecular weight [35] and the calculated radii of gyration for the different tracers $R_g^2 = l_{seg}^2 N/6$ with $l_{seg} = 0.568\, nm$ [36]

Sample	M_n [kg/mol]	N	M_w/M_n	M_n/M_e	R_g [nm]
PEO1K	1.00	23	1.04	0.48	1.11
PEO2K	2.11	48	1.04	1.0	1.60
PEO3K	3.16	71	1.07	1.5	1.95
PEO4K	4.53	103	1.03	2.2	2.35

Methods. Applying neutron wavelengths of λ=1.0 and 1.35 nm the experiments were performed using the IN15 neutron spin echo (NSE) instrument at the Institut Laue-Langevin (ILL) in Grenoble. At T=413 K, spanning a time range 0.3 ns $\leq t \leq$ 500 ns, we covered a range of momentum transfers 0.5 nm^{-1} $\leq Q \leq$ 1.2 nm^{-1}. For the PEO4K tracer also the dynamics at T=464 K was studied. The experimental results were corrected for background and resolution. For a short chain in a long entangled slowly moving matrix also the slow dynamics indirectly contributes to the observed spectra. In order to perform the necessary dynamic RPA corrections, the pure long chain matrix containing 5% hydrogenous chains was also investigated at 413 and 464 K and fitted with an interpolation function as described in Ref. [33]. Finally, to investigate, whether the NSE determined Fickian diffusion coefficients agree with macroscopic diffusion, we also undertook PFG-NMR measurements on the PEO2K, PEO3K and PEO4K samples [†] that were studied before with neutrons (see SI).

[†] The PEO1K sample was not available for PFG NMR measurements.

Experimental results

We have studied the molecular weight-dependent dynamic structure factors from hydrogen-labelled PEO tracer chains in a deuterated high molecular weight PEO melt. The investigation was performed on samples with altogether 4 different tracer molecular weights (see Table 1). Figure 1 displays the measured NSE spectra for all tracers in the deuterated PEO matrix at 413K.

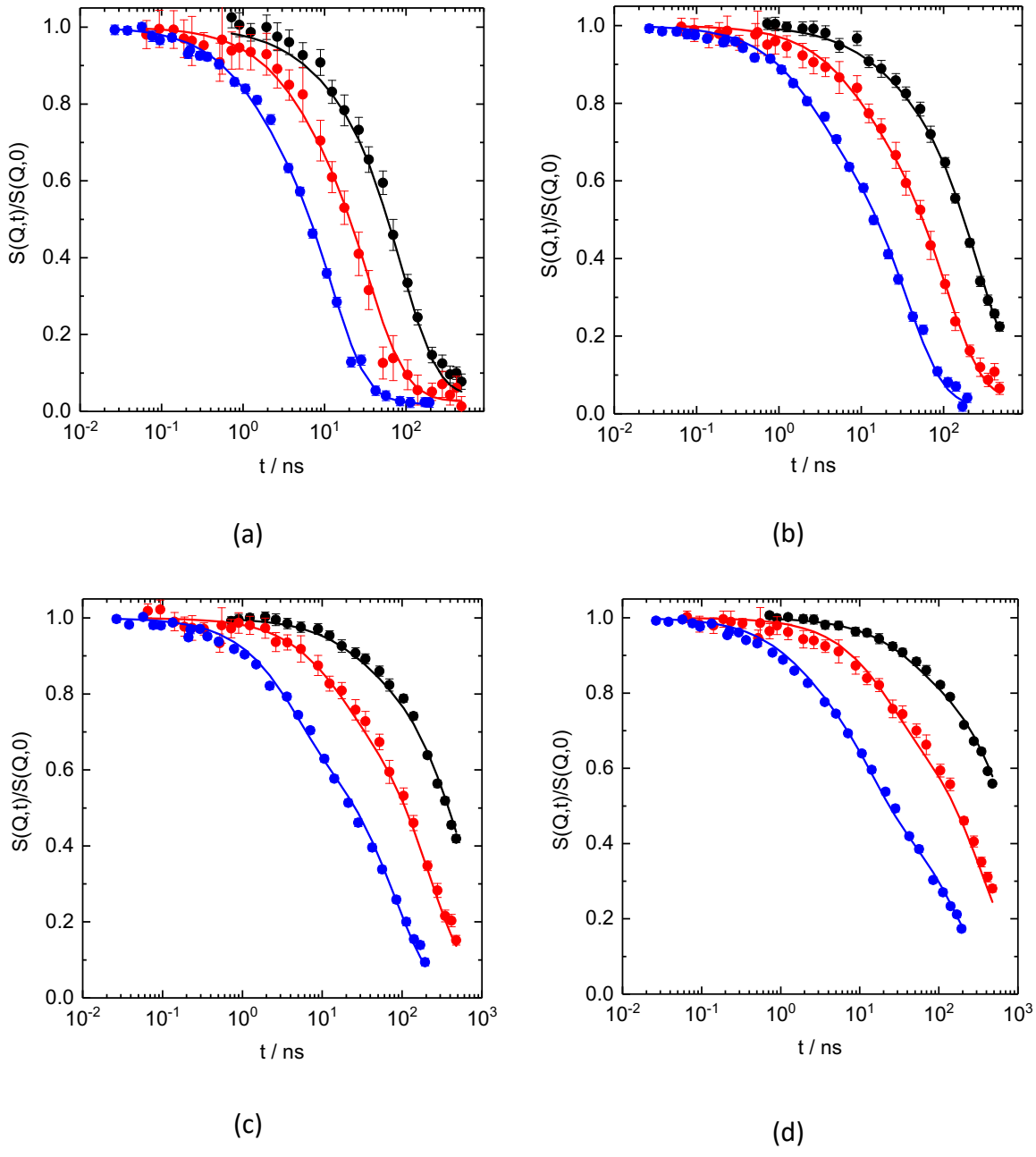

Figure 1: NSE spectra from all tracers: PEO1K (a), PEO2K (b), PEO3K (c), PEO4K (d) tracers in the deuterated PEO matrix; Q-values from above 0.5 nm^{-1} (black); 0.8 nm^{-1} (red) and 1.2 nm^{-1} (blue). The lines display the result of the joint fit of all spectra (see text).

The spectra displayed in Figure 1 result from a combination of center-of-mass mean squared displacements $\langle r_{com}^2(t)\rangle$, Rouse mode contributions and contributions from the host dynamics via dynamic RPA.

NG-behavior is governed by the α_2(t) function (Equ. 7) containing 3 parameters: its magnitude α_0, the position of its maximum $t_{max}{\sim}\tau_R$ and its width σ. For the segment MSD (Equ. 5a) as well as the Rouse contribution (Equ. 5b) all parameters are known [37]. We fitted all spectra with the scattering function of Equ. 3 combining the contributions from the Rouse motion, the Non-Gaussianity and the corrections for dynamic RPA.

In order to quantify the RPA correction in terms of a correction function we used the following procedure. The NSE data were fitted to a model function that comprises the internal Rouse dynamics including NG corrections (Equs. 3-4). The ratio of the computed functions as fitted with RPA and calculated without RPA yields the correction function for the experimental data. Since the application of the dynamical RPA also requires the scattering function of the long matrix as input, these are represented by an interpolation Ansatz (Ref. [33]) that perfectly describes all previously known NSE data from long chains over the complete available time and Q-range.

Scrutinizing the NG-model established by Equs. 3-7 it is unavoidable to deal with a significant number of parameters and therefore it is essential to use all prior information available. (i)

The structural and Rouse parameters are known from earlier experiments on PEO at the same temperature: $Wl_{seg}^4 = 1.489\ \frac{\mathrm{nm}^4}{\mathrm{ns}}$ [37]; the segment length $l_{seg} = 0.568\ \mathrm{nm}$ [36]; (ii) the tube diameter of highly entangled PEO $d_{tube} = 4.75\ \mathrm{nm}$ [37]; (iii) tracer diffusion coefficients for PEO2K, PEO3K and PEO4K at 413 K were obtained from PFG-NMR studies (Table 2 and Figs. S2 and S3). (iv) Following Guenza-model [27] the maxima of the NG-correction appears at $t_{max} \cong \tau_R$ that given the Rouse parameters are at hand (Table 2); (v) finally, the strength of $\alpha_2(t), \alpha_0$ is expected to be independent of the tracer length – the tracers are supposed to mirror the dynamics of always the same host.

With this knowledge a first joint fit of all spectra from the 4 tracers (altogether 12 spectra) was undertaken: Variables were the parameters determining $\alpha_2(t)$; thereby the strength parameter α_0 was taken as equal for all tracers; t_{max} was set proportional to the Rouse times with one common proportionality factor t_{max}^0; the width parameter σ was also set equal for all tracers. As further parameter the slopes in the sub-diffusive regime β and the cross over mean square displacement $\langle r_{cross}^2 \rangle$ were fitted. With this first approach already a very reasonable fit was achieved (residual sum of errors $\chi^2 = 1.55$) that resulted in ($\alpha_0 = 0.214 \pm 0.007$; $t_{max}^0 = 2.56 \pm 0.35\ \mathrm{ns}$; $\sigma = 2.18 \pm 0.13$; $\langle r_{cross}^2 \rangle = 17.5 \pm 0.9\ \mathrm{nm}^2$) the stretching parameters from short to long tracers became $\beta = 0.79 \pm 0.01,\ 0.74 \pm 0.01,\ 0.72 \pm 0.01,\ 0.65 \pm 0.01$. In the following steps the parameters were refined: (1) the Fickian diffusion coefficient at constant α_0 were allowed to vary, Table 2 displays the results that all are very close to the PFG-NMR results taken at a very different time and length scale (hundreds of ms and μm). Varying the Fickian-diffusion coefficients improved χ^2 to 1.35. Their dependence on the tracer length together with the NMR-results is displayed in Figure 2. (2) The dependence of α_0 on the tracer length N was investigated. The results are shown in the bottom left insert

of Figure 2, where χ^2 as a function of the exponent *x* in $\alpha_0 \sim N^x$ is displayed. Indeed χ^2 assumes a minimum at x = 0 as expected from the Guenza model. (3) We studied, how the χ^2 evolved for different prescribed values for $\langle r_{cross}^2 \rangle$. The result is shown as a second upper right insert in Figure 2. Finally, the solid lines in Figure 1 display the achieved quality of data description by our fitting strategy. We note that even at Q=1.2 nm^{-1}, where without the NG corrections the Rouse mode contribution would be very large (Figure S4), we get an excellent data description over the whole NSE time range.

Table 2: Rouse diffusion coefficients D_R; tracer diffusion coefficients within the 40K host: obtained by PFG-NMR, D_{tr} [NMR] and NSE, D_{tr} [NSE]; the tracer's Rouse times τ_R; the times, t_{max}, where the $\alpha_2(t)$ assume their maxima and the slopes β in the sub-diffusive regime.

Sample	N	D_R $10^2 \left[\frac{nm^2}{ns}\right]$	D_{tr} [NMR] $10^2 \left[\frac{nm^2}{ns}\right]$	D_{tr} [NSE] $10^2 \left[\frac{nm^2}{ns}\right]$	τ_R [ns]	t_{max}[ns]	β
PEO1K	23	6.69	-	4.78 ± 0.13	3.75	3.15	0.79 ± 0.01
PEO2K	48	3.21	1.62 ± 0.13	1.59 ± 0.02	16.3	13.7	0.74 ± 0.008
PE03K	71	2.16	0.78 ± 0.06	0.74 ± 0.01	35.7	30.0	0.71 ± 0.009
PEO4K	103	1.49	0.40 ± 0.02	0.44 ± 0.008	75.1	63.2	0.68 ± 0.01
PEO4K (T=464K)	103	3.36	0.98 ± 0.05	1.02 ± 0.02	33.3	27.8 fixed	0.60 ± 0.007

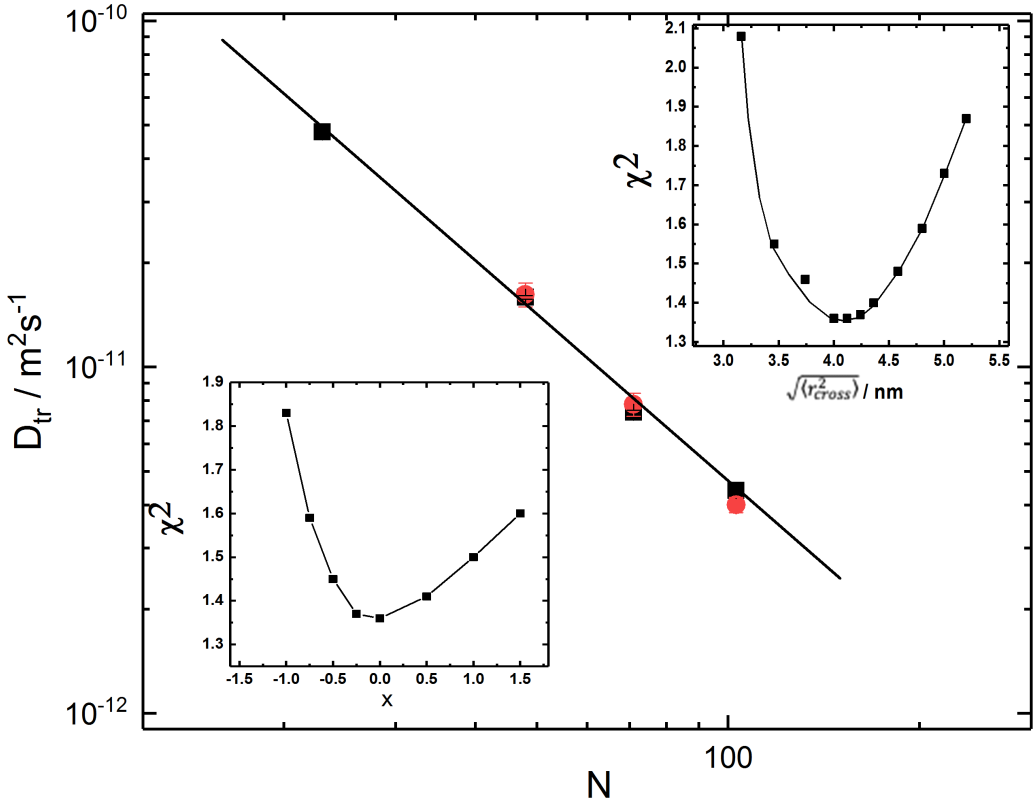

Figure 2: Fickian diffusion coefficients $D_{tr}(N)$ from PFG-NMR (circles) and NSE (squares) in a double logarithmic presentation as a function of tracer length *N*. Residual sum of errors χ^2 for a joint fit of all spectra as a function of the power law exponent *x* for (i) the strength of the NG contribution $\alpha_0 \sim N^x$; (bottom left insert); (ii) for the cross over length $\sqrt{\langle r_{cross}^2 \rangle}$ (upper right insert). Solid line shows fit with power law $D_{tr}(N) \sim N^{-1.61 \pm 0.04}$

Last but not least it was an important task of our study on PEO to find out, to what extent the PE result of cooperative dynamics within the entanglement volume is valid also for PEO, which compared to PE constitutes a chemically quite different polymer featuring an oxygen in the backbone. In order to obtain the center-of-mass tracer $\langle r_{com}^2(t) \rangle$, we need to correct the experimental data for dynamic random phase approximation (RPA) and the contributions from the internal Rouse modes modified by the NG corrections. The procedure is described in detail in the SI. The $\langle r_{com}^2(t) \rangle$ then are calculated from an inversion of the normalized and corrected dynamic structure factor

$$S_{corr}(Q,t) = exp\left[-\frac{Q^2}{6}\langle r_{com}^2(t)\rangle\right] \quad (9)$$

$$\langle r_{com}^2(t)\rangle = -\frac{6}{Q^2} ln[S_{corr}(Q,t)] \quad (10)$$

Figure 3 displays the obtained $\langle r_{com}^2(t)\rangle$ for the different tracers. Like the PE tracers, the PEO1K, PEO2K and PEO3K chains exhibit a sub-diffusive regime at shorter times that crosses over to Fickian diffusion beyond a threshold $\langle r_{cross}^2\rangle$. The dashed lines indicate the $MSD_{NMR}(t)$ calculated on the basis of the PFG-NMR data (see Table 2). As may be seen, they very nicely agree with the NSE derived $\langle r_{com}^2(t)\rangle$ beyond $\langle r_{cross}^2\rangle$. For the longest tracer PEO4K within the dynamical window of NSE the observed center-of-mass displacement remains sub-diffusive. Following the NMR result the cross over time would be expected at about 800 ns.

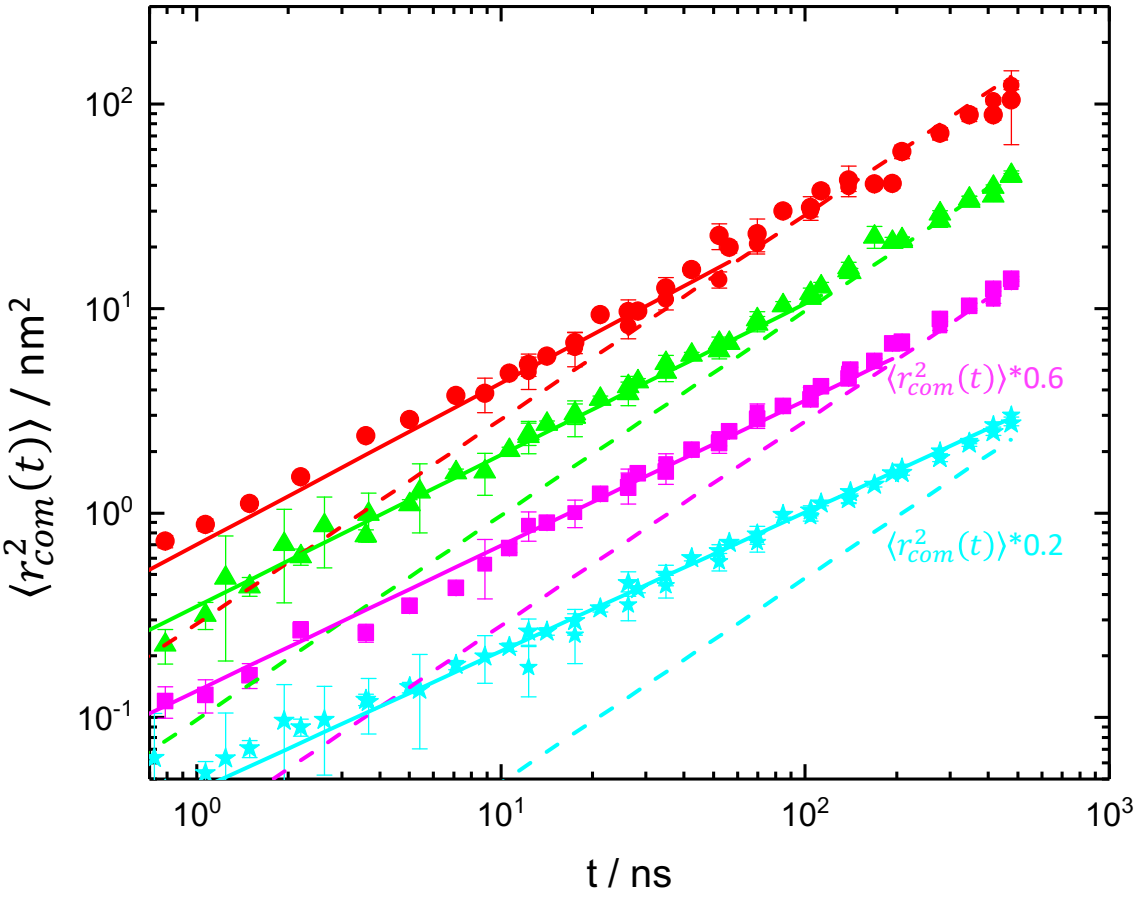

Figure 3: $\langle r_{com}^2(t)\rangle$ for the different tracers from PEO1K (red circles), PEO2K (green triangles), PEO3K (magenta squares) and PEO4K (cyan stars) calculated from the NSE scattering curves measured for Q=0.8 nm^{-1} and 1.2 nm^{-1} at 413K. The curves for PEO3K and PEO4K are shifted by factors 0.6 and 0.2 respectively. For PEO2K, PEO3K and PEO4K the dashed lines indicate Fickian diffusion ($\langle r_{com}^2(t)\rangle \sim t$) as derived from the PFG-NMR results. Solid lines represent fits to the sub-diffusive part.

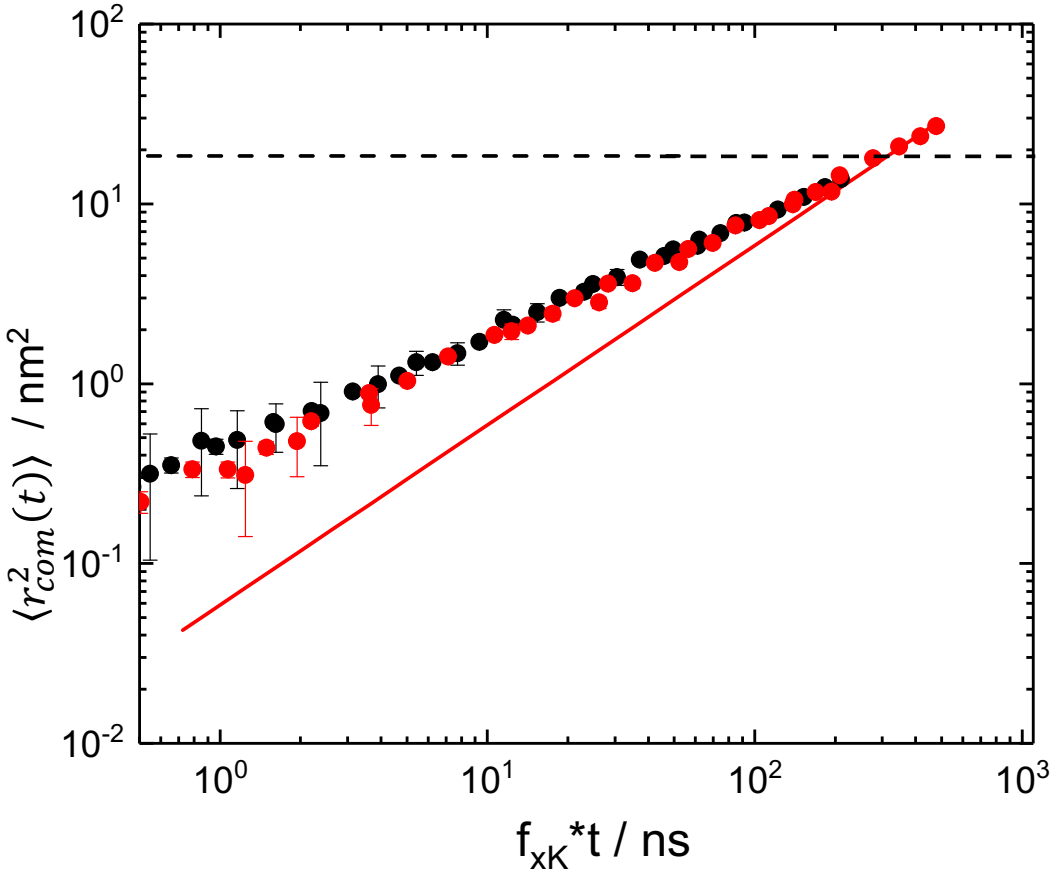

Figure 4: Combination of $\langle r_{com}^2(t)\rangle$ derived from the measurements on the PEO4K sample at 2 different temperatures, 413K (black circle) and 464K (red circle). The abscissa represents the time scaled with a factor $f_{xK} = D_{xK}/D_{464K}$. The scaling factors f_{xK} are D_{464K}/D_{464K}: 1 D_{413K}/D_{464K}: 0.44. The solid line shows the Fickian diffusion ($\langle r_{com}^2(t)\rangle \sim t$), the dashed line indicates the cross-over point $\langle r_{cross}^2\rangle$ at 17.5 nm^2 (for the details see the main text).

In order to visualize the Fickian regime also for this tracer, we performed an additional experiment at T=464 K. We compare the T=464 K data with those from T=413 K, by scaling the time axis with the ratio of the Fickian diffusion coefficients at the two temperatures. The Fickian diffusion coefficient at 413K was obtained by PFG-NMR (see SI). The scaling factor f_{xK} results from the known temperature dependence of the Rouse variable Wl_{seg}^2, which is in accordance with various macroscopic measurements [35]. The scaling plot displayed in Figure 4 now also for the PEO4K sample shows the cross over from sub-diffusion to Fickian diffusion.

Discussion

Non-Gaussianity. Non-Gaussian dynamics of segment motion means that the distribution of segmental displacements does not follow the Gaussian form. Depending on the sign of $\alpha_2(t)$ the distribution might become broader or narrower than the corresponding Gaussian distribution. In general terms, for a negative $\alpha_2(t)$ the distribution in "real space" becomes broader than a Gaussian. Thus, some displacements are larger and others are smaller than a Gaussian distribution would dictate. We note that the sign of $\alpha_2(t)$ is positive for all tracers. Then the opposite holds: at the degree of approximation the distribution in "Q-space" gets broader, with the consequence that in real space the displacement distribution will be narrower than a Gaussian. Thus, in our case of a positive $\alpha_2(t)$ that goes along with the Q^4 term in the scattering function, the distribution in real space narrows down. With such a positive $\alpha_2(t)$–function, we are able to successfully fit the scattering data obtained from all tracers in a global fit. The narrower distribution function implies that larger deviations from the average displacements are reduced. We hypothesize that the tube confinement of the matrix reduces larger runaway displacements relative to the average displacement.

Now we compare our results with the quantitative predictions by Guenza. On the one hand we observe that her finding $t_{max}(N) \approx \tau_R(N)$ is in perfect agreement with our results, even though, as it turns out the fit is not very sensitive to the exact exponent x in $t_{max} \sim N^x$ (see Figure S5). Furthermore, the fit reveals that with good accuracy the strength parameter α_0 is independent of the tracer's length. In order to investigate the N-dependence in more detail we evaluated χ^2 for different fixed values of the power law exponent x in $\alpha_0 \sim N^x$. The insert in Figure 2 shows the result: χ^2 exhibits an asymmetric minimum around $x = 0$. On the right side χ^2 exhibits a nearly linear increase indicating some leverage for $x > 0$. On the left side χ^2 increases quadratically showing that negative x values are rather excluded. Thus, the NG-

correction appears to be independent of x. As the cooperativity of tracer motions with the host shows, the tracers mirror the host dynamics within the tube. Then, given the fact, that the host is always the same highly entangled 40K PEO, a constant strength $\alpha_0\ (N)$ is expected from Guenza's approach and further supports the notion of cooperative motion with the host. The behavior of the normalized sum of squared errors χ^2 on different parameter planes are shown in the SI (Figs. S6 and S7)

MSD. We now inspect the experimental results on the center-of-mass displacements for the different tracers. Figure 5 displays the $\langle r_{com}^2(t)\rangle$ for the different tracer lengths in a master plot, where the time axis was scaled with a factor $f_{PEOxK} = D_{PEOxK}/D_{PEO1K}$. As in PE, we observe sub-diffusive displacements at shorter times that for all tracers cross over to a linear time dependence at the same $\langle r_{com}^2(t)\rangle$ =$\langle r_{cross}^2\rangle = 17.5\ \mathrm{nm}^2$. The position of the cross over is indicated by horizontal line. $\sqrt{\langle r_{cross}^2\rangle} = 4.2\ \mathrm{nm}$ is very close to the entanglement distance or tube diameter in strongly entangled PEO melts, where by NSE $d_{tube} = 4.75\ \mathrm{nm}$ was found [37]. The range of sub-diffusive behavior is not determined by the size of the tracer but for all tracers in an equal fashion given by the lateral dimension of the confining tube of the entangled host. Thus, as shown and discussed for PE, also in highly entangled PEO melts the tracer's monomers interact strongly with the host and move cooperatively with the host segments. Decorrelation is determined by the host and occurs, whenever the $\langle r_{com}^2(t)\rangle$ has reached a value close to the lateral tube size - cooperativity is limited by the entanglement volume. As already noted for PE, the cooperative segment motion within the entanglement volume contradicts the assumption of independent chain motion (Rouse dynamics) within the tube that is one basic element of the reptation model.

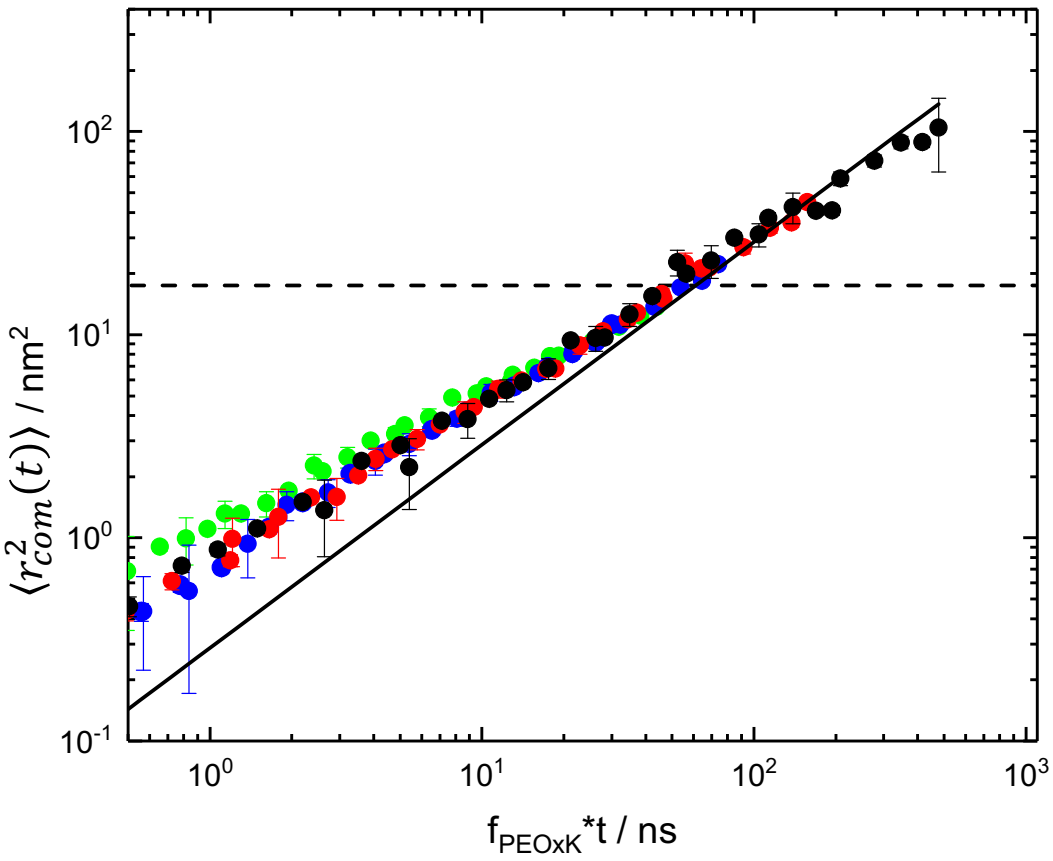

Figure 5: Centre-of-mass $\langle r_{com}^2(t)\rangle$ for the different PEO tracers with the time axis scaled with a factor proportional to the respective Fickian diffusion coefficients. The solid line shows the Fickian diffusion law $\sim t$, the dash line indicates the cross-over point $\langle r_{cross}^2\rangle$ at 17.5 nm^2 (for the details see the text); Black: PEO1K; red: PEO2K; blue: PEO3K; green: PEO4K. The scaling factors f_{PEOxK} are D_{PEO2K}/D_{PEO1K}: 0.33; D_{PEO3K}/D_{PEO1K}: 0.16; D_{PEO4K}/D_{PEO1K}: 0.092.

Fickian diffusion: The tracer diffusion coefficients decrease with increasing N as $D_{tr}(N)\sim N^{-1.61\pm0.04}$ somewhat less pronounced than for similar chain lengths of PE ($N^{-1.85}$). We note that by MD simulation on coarse grained chains for the motion of short dilute unentangled tracers of length N in an entangled matrix Durand *et al.* [38] found the Rouse diffusion law $D_{tr} \sim N^{-1}$ for the entire range of N. The observation of Fickian diffusion that does not follow the Rouse prediction $D = \frac{k_B T}{N\zeta}$, where ζ is the monomeric friction coefficient implies that the monomeric friction alone is not determining center-of-mass diffusion. This non-Rouse N-dependence for dilute tracer chains immersed in a highly

entangled host was already observed a long time ago by macroscopic scanning infrared microscopy measurements [39]. As we have shown on PE tracers our results for the Fickian diffusion coefficient beyond the cross over from sub-diffusivity quantitatively agree with these macroscopic results [28]. Thus, it is not surprising to find a similar result for PEO tracers. Since the results on the nanometer scale quantitatively agree with macroscopic studies (PE) and measurements on the micrometer scale (PEO), there appears to be no further mechanism that affects the tracer diffusion beyond the nm scale. Then, the steeper N-dependence of the Fickian diffusion must be related to a scale dependent viscosity of the host matrix that differs from the Rouse-like viscosity of the tracer chains in their own equivalent melt. Apparently, the scale for establishing this viscosity is that of the tube. Finally, we note that the cross over time $\tau_{cross} = \langle r_{cross}^2 \rangle / (6D_{tr})$ is not related to the internal dynamics of the tracers that is characterized by the respective Rouse times τ_R. Both scale differently with the tracer length $\tau_{cross} \sim \frac{1}{D_{tr}} \sim N^{1.61}$ and $\tau_R \sim N^2$. This behavior differs from the dynamics of Rouse chains, where $\tau_{cross} \cong \tau_R$ [28].

Conclusion

In conclusion, we summarize our results and emphasize their importance for future more fundamental approaches to rationalize the reptation idea on a molecular basis:

- As in the earlier investigation on PE [28] we have found that short tracer chains in a highly entangled PEO matrix perform anomalous sub-diffusion that is dictated by the host and limited by the entanglement volume – the tracers move cooperatively with the host.
- For all tracers the strength of the NG correction $\alpha_0(N)$ is equal. The independence of the NG corrections from the tracer length is another proof that the tracers mirror the host dynamics, which does not depend on the tracer length.

- The magnitude of the NG correction $\alpha_0(N) \sim \sqrt{N}$ proposed by Guenza is not found, because we observe the image of the host dynamics; for all tracers the host was the same.
- We hypothesize that the cross over to Fickian diffusion at $\langle r_{cross}^2 \rangle \cong d^2$ indicates that beyond the entanglement volume not only the cooperativity is lifted but also the NG displacement distribution is averaged leading to the generic Gaussian distributed MSD valid for diffusion.
- The Fickian-diffusion observed at the nm–scale agrees quantitatively with the macroscopic (PE) and mesoscopic diffusion (PEO). On the other hand, its dependence on the tracer length deviates strongly from the Rouse prediction ($D \sim \frac{1}{N}$) indicating that it is governed by a non-local viscosity established on the scale of the tube.
- The Non-Gaussianity is also the physical reason for the observed weak Rouse contributions to the dynamic structure factor of tracer chains in long chain melts. The effect was already observed for PE tracers in strongly entangled PE melts but so far remained unexplained.

As a final conclusion our experiment together with the earlier observations on PE [28] clearly reveals that as a generic feature in highly entangled polymer melts the **dynamics within the tube is not only cooperative but also significantly Non-Gaussian.** These phenomena will need to be considered in developing molecular theories underpinning the reptation idea.

Acknowledgement: We acknowledge ILL for granting the beam time for the NSE measurements and express our gratitude to Marina Guenza for important discussions. The raw data of the NSE experiment can be found at dx.doi./10.5291/ILL-DATA.CRG-2804.

Supporting information: determination of MSD, PFG-NMR, RPA correction, residual error maps.

References

(1) Di, X.; McKenna, G. B. Evaluation of Heterogeneity Measures and Their Relation to the Glass Transition. *J. Chem. Phys.* **2013**, *138* (12), 12A530 DOI: 10.1063/1.4779057.

(2) Ottochian, A.; De Michele, C.; Leporini, D. Non-Gaussian Effects in the Cage Dynamics of Polymers. *Philos. Mag.* **2008**, *88* (33–35), 4057–4062 DOI: 10.1080/14786430802348060.

(3) Henritzi, P.; Bormuth, A.; Klameth, F.; Vogel, M. A Molecular Dynamics Simulations Study on the Relations between Dynamical Heterogeneity, Structural Relaxation, and Self-Diffusion in Viscous Liquids. *J. Chem. Phys.* **2015**, *143* (16), 164502 DOI: 10.1063/1.4933208.

(4) Pan, D.; Sun, Z. Y. Influence of Chain Stiffness on the Dynamical Heterogeneity and Fragility of Polymer Melts. *J. Chem. Phys.* **2018**, *149* (23), 234904 DOI: 10.1063/1.5052153.

(5) Ye, Y.; Qin, H.; Tian, M.; Mi, J. G. Diffusion Mode Transition between Gaussian and Non-Gaussian of Nanoparticles in Polymer Solutions. *Chinese J. Polym. Sci. (English Ed.* **2019**, *37* (7), 719–728 DOI: 10.1007/s10118-019-2237-9.

(6) Pan, D.; Sun, Z.-Y. Diffusion and Relaxation Dynamics of Supercooled Polymer Melts. *Chinese J. Polym. Sci. 2018 3610* **2018**, *36* (10), 1187–1194 DOI: 10.1007/S10118-018-2132-9.

(7) Arbe, A.; Colmenero, J.; Alvarez, F.; Monkenbusch, M.; Richter, D.; Farago, B.; Frick, B. Non-Gaussian Nature of the [Formula Presented] Relaxation of Glass-Forming Polyisoprene. *Phys. Rev. Lett.* **2002**, *89* (24), 245701 DOI: 10.1103/PhysRevLett.89.245701.

(8) Khairy, Y.; Alvarez, F.; Arbe, A.; Colmenero, J. Disentangling Self-Atomic Motions in Polyisobutylene by Molecular Dynamics Simulations. *Polymers (Basel).* **2021**, *13* (4), 1–23 DOI: 10.3390/polym13040670.

(9) Aichele, M.; Gebremichael, Y.; Starr, F. W.; Baschnagel, J.; Glotzer, S. C. Polymer-Specific Effects of Bulk Relaxation and Stringlike Correlated Motion in the Dynamics of a Supercooled Polymer Melt. *J. Chem. Phys.* **2003**, *119* (10), 5290–5304 DOI: 10.1063/1.1597473.

(10) Pazmiño Betancourt, B. A.; Douglas, J. F.; Starr, F. W. Fragility and Cooperative Motion in a Glass-Forming Polymer-Nanoparticle Composite. *Soft Matter* **2013**, *9* (1), 241–254 DOI: 10.1039/c2sm26800k.

(11) Xu, W.-S.; Douglas, J. F.; Freed, K. F. Influence of Pressure on Glass Formation in a Simulated Polymer Melt. *Macromolecules* **2017**, *50* (6), 2585–2598 DOI: 10.1021/ACS.MACROMOL.7B00080.

(12) Doi, M.; S.F.Edwards. *The Theory of Polymer Dynamics*; Clarendon press Oxford: Oxford, 1986.

(13) Zamponi, M.; Weschnewski, A.; Monkenbusch, M.; Willner, L.; Richter, D.; Falus, P.; Farago, B.; Guenza, M. G. Cooperative Dynamics in Homopolymer Melts: A Comparison of Theoretical Predictions with Neutron Spin Echo Experiments. *J. Phys. Chem. B* **2008**, *112* (50), 16220–16229 DOI: 10.1021/jp807035z.

(14) Smith, G. D.; Paul, W.; Monkenbusch, M.; Richter, D. On the Non-Gaussianity of Chain

Motion in Unentangled Polymer Melts. *J. Chem. Phys.* **2001**, *114* (9), 4285–4288 DOI: 10.1063/1.1348032.

(15) Paul, W.; Smith, G. D.; Yoon, D. Y.; Farago, B.; Rathgeber, S.; Zirkel, A.; Willner, L.; Richter, D. Chain Motion in an Unentangled Polyethylene Melt: A Critical Test of the Rouse Model by Molecular Dynamics Simulations and Neutron Spin Echo Spectroscopy. *Phys. Rev. Lett.* **1998**, *80* (11), 2346–2349 DOI: 10.1103/PhysRevLett.80.2346.

(16) Smith, G. D.; Paul, W.; Monkenbusch, M.; Richter, D. A Comparison of Neutron Scattering Studies and Computer Simulations of Polymer Melts. *Chem. Phys.* **2000**, *261* (1–2), 61–74 DOI: 10.1016/S0301-0104(00)00228-7.

(17) Karayiannis, N. C.; Giannousaki, A. E.; Mavrantzas, V. G.; Theodorou, D. N. Atomistic Monte Carlo Simulation of Strictly Monodisperse Long Polyethylene Melts through a Generalized Chain Bridging Algorithm. *J. Chem. Phys.* **2002**, *117* (11), 5465 DOI: 10.1063/1.1499480.

(18) Karayiannis, N. C.; Mavrantzas, V. G.; Theodorou, D. N. A Novel Monte Carlo Scheme for the Rapid Equilibration of Atomistic Model Polymer Systems of Precisely Defined Molecular Architecture. *Phys. Rev. Lett.* **2002**, *88* (10), 105503 DOI: 10.1103/PhysRevLett.88.105503.

(19) Kreer, T.; Baschnagel, J.; Müller, M.; Binder, K. Monte Carlo Simulation of Long Chain Polymer Melts: Crossover from Rouse to Reptation Dynamics. *Macromolecules* **2001**, *34* (4), 1105–1117 DOI: 10.1021/ma001500f.

(20) Padding, J. T.; Briels, W. J. Uncrossability Constraints in Mesoscopic Polymer Melt Simulations: Non-Rouse Behavior of C120H242. *J. Chem. Phys.* **2001**, *115* (6), 2846–2859 DOI: 10.1063/1.1385162.

(21) Kremer, K.; Grest, G. S. Dynamics of Entangled Linear Polymer Melts: A Molecular-Dynamics Simulation. *J. Chem. Phys.* **1990**, *92* (8), 5057–5086 DOI: 10.1063/1.458541.

(22) Guenza, M. Many Chain Correlated Dynamics in Polymer Fluids. *J. Chem. Phys.* **1999**, *110* (15), 7574–7588 DOI: 10.1063/1.478660.

(23) Guenza, M. Intermolecular Effects in the Center-of-Mass Dynamics of Unentangled Polymer Fluids. *Macromolecules* **2002**, *35* (7), 2714–2722 DOI: 10.1021/ma011596t.

(24) Guenza, M. Cooperative Dynamics in Unentangled Polymer Fluids. *Phys. Rev. Lett.* **2002**, *88* (2), 4 DOI: 10.1103/PhysRevLett.88.025901.

(25) Guenza, M. Cooperative Dynamics in Semiflexibile Unentangled Polymer Fluids. *J. Chem. Phys.* **2003**, *119* (14), 7568–7578 DOI: 10.1063/1.1606674.

(26) Sambriski, E. J.; Yatsenko, G.; Nemirovskaya, M. A.; Guenza, M. G. Bridging Length Scales in Polymer Melt Relaxation for Macromolecules with Specific Local. *J. Phys. Condens. Matter* **2007**, *19* (20), 205115 DOI: 10.1088/0953-8984/19/20/205115.

(27) Guenza, M. G. Localization of Chain Dynamics in Entangled Polymer Melts. *Phys. Rev. E - Stat. Nonlinear, Soft Matter Phys.* **2014**, *89* (5), 052603 DOI: 10.1103/PhysRevE.89.052603.

(28) Zamponi, M.; Kruteva, M.; Monkenbusch, M.; Willner, L.; Wischnewski, A.; Hoffmann, I.; Richter, D. Cooperative Chain Dynamics of Tracer Chains in Highly Entangled Polyethylene Melts. *Phys. Rev. Lett.* **2021**, *126* (18), 187801 DOI: 10.1103/PhysRevLett.126.187801.

(29) Farago, J.; Semenov, A. N.; Meyer, H.; Wittmer, J. P.; Johner, A.; Baschnagel, J. Mode-Coupling Approach to Polymer Diffusion in an Unentangled Melt. I. the Effect of Density Fluctuations. *Phys. Rev. E - Stat. Nonlinear, Soft Matter Phys.* **2012**, *85* (5), 051806 DOI: 10.1103/PhysRevE.85.051806.

(30) Richter, D.; Monkenbusch, M.; Arbe, A.; Colmenero, J. Neutron Spin Echo in Polymer Systems. *Adv. Polym. Sci.* **2005**, *174*, 1 DOI: 10.1007/b106578.

(31) Colmenero, J. The Universal Trend of the Non-Exponential Rouse Mode Relaxation in Polymer Systems: A Theoretical Interpretation Based on a Generalized Langevin Equation. *Soft Matter* **2015**, *11* (28), 5614–5618 DOI: 10.1039/c5sm00790a.

(32) Akcasu, A. Z.; Tombakoglu, M. Dynamics of Copolymer and Homopolymer Mixtures in Bulk and in Solution via the Random Phase Approximation. *Macromolecules* **1990**, *23* (2), 607–612 DOI: 10.1021/ma00204a038.

(33) Monkenbusch, M.; Kruteva, M.; Zamponi, M.; Willner, L.; Hoffman, I.; Farago, B.; Richter, D. A Practical Method to Account for Random Phase Approximation Effects on the Dynamic Scattering of Multi-Component Polymer Systems. *J. Chem. Phys.* **2020**, *152* (5), 054901 DOI: 10.1063/1.5139712.

(34) Hövelmann, C. H.; Gooßen, S.; Allgaier, J. Scale-Up Procedure for the Efficient Synthesis of Highly Pure Cyclic Poly(Ethylene Glycol). *Macromolecules* **2017**, *50* (11), 4169–4179 DOI: 10.1021/acs.macromol.7b00361.

(35) Niedzwiedz, K.; Wischnewski, A.; Pyckhout-Hintzen, W.; Allgaier, J.; Richter, D.; Faraone, A. Chain Dynamics and Viscoelastic Properties of Poly(Ethylene Oxide). *Macromolecules* **2008**, *41* (13), 4866–4872 DOI: 10.1021/ma800446n.

(36) Kruteva, M.; Allgaier, J.; Monkenbusch, M.; Porcar, L.; Richter, D. Self-Similar Polymer Ring Conformations Based on Elementary Loops: A Direct Observation by SANS. *ACS Macro Lett.* **2020**, *9* (4), 507–511 DOI: 10.1021/acsmacrolett.0c00190.

(37) Gold, B. J.; Pyckhout-Hintzen, W.; Wischnewski, A.; Radulescu, A.; Monkenbusch, M.; Allgaier, J.; Hoffmann, I.; Parisi, D.; Vlassopoulos, D.; Richter, D. Direct Assessment of Tube Dilation in Entangled Polymers. *Phys. Rev. Lett.* **2019**, *122* (8), 088001 DOI:

10.1103/PhysRevLett.122.088001.

(38) Durand, M.; Meyer, H.; Benzerara, O.; Baschnagel, J.; Vitrac, O. Molecular Dynamics Simulations of the Chain Dynamics in Monodisperse Oligomer Melts and of the Oligomer Tracer Diffusion in an Entangled Polymer Matrix. *J. Chem. Phys.* **2010**, *132* (19), 194902 DOI: 10.1063/1.3420646.

(39) Seggern, J. Von; Klotz, S.; Cantow, H. J. Reptation and Constraint Release in Linear Polymer Melts: An Experimental Study. *Macromolecules* **2002**, *24* (11), 3300–3303 DOI: 10.1021/MA00011A039.